Journal of Chemical Engineering of Japan, Vol. 40, No. 4, pp. 304–311, 2007 **Research Paper**

CFD Simulation of the Flow Pattern for Drag Reducing Fluids in Turbulent Pipe Flows

Mahesh T. DHOTRE, Kalekudithi EKAMBARA
and Jyeshtharaj B. JOSHI
Institute of Chemical Technology, University of Mumbai, Matunga, Mumbai-400019, India

Keywords: Drag Reduction, Pipe Flow, Turbulence, CFD and Low Reynolds Number k–ε Model

In the present work, the flow pattern in pipe flows has been simulated for drag reducing fluids using a low Reynolds number k–ε model. The model uses a non-linear molecular viscosity and damping function to account for near wall effects. The comparison between the predictions and the experimental profiles of axial velocity and kinetic energy are in good agreement. A systematic study has been undertaken to investigate the effect of rheological parameters and to consider the modification to the flow that arises in the presence of a fluid yield stress.

Introduction

The flow of non-Newtonian fluids and slurries in pipes occurs in a wide range of practical applications in the process industries. Most flows of engineering importance are turbulent and viscosities must be high before a laminar flow predominates. When viscosities are high the fluids are often non-Newtonian in character. Thus, in the field of the non-Newtonian flow, the laminar flow tends to predominate. However, there are still many instances in which the turbulent flow of non-Newtonian fluids is encountered. This non-Newtonian behavior may be an inherent property of the material or may have resulted from the use of additives to achieve particular rheological characteristics. The addition of very small concentrations of high polymeric substances can reduce the frictional resistance in the turbulent flow to as low as one-quarter that of the pure solvent. This phenomenon, drag reduction, can occur both with fluids which exhibit Newtonian and non-Newtonian viscous characteristics.

Extensive experimental and theoretical studies of turbulent non-Newtonian pipe flows were carried out by Metzner and co-workers during the 1950s (Metzner and Reed, 1955; Metzner, 1957; Dodge and Metzner, 1959). These workers indicated how the friction factor f varies with a generalized Reynolds number Re (Metzner and Reed, 1955) in the laminar, transitional and turbulent regimes. For the fully-developed turbulent flow of power-law fluids, Dodge and Metzner (1959) developed a semi-theoretical expression for the mean velocity profile together with a correlation for f versus Re. The study revealed that a decreasing n slightly delays transition to higher Re, and that friction factors reduce with decreasing values of n. Hartnett and Kostic (1990) examined the available turbulent friction-factor correlations, and found that the Dodge and Metzner correlation (1959) produced the best agreement with the available measurements. The transition regime has been considered by Reed and Pilehvari (1993) who developed a procedure to calculate transitional friction factors by combining the laminar and turbulent friction factors of Dodge and Metzner (1959).

Mohammed *et al*. (1975) developed a method for calculating the fully-developed friction factor and mean velocity profile by numerical integration of the mean-momentum equation. The Reynolds stresses were modeled by analogy with the power-law model, and by use of Prandtl's hypothesis (Schlichting, 1968). Their calculations showed fairly good agreement with the measurements of Bogue (1959) over a wide range of Re and n, although the model coefficients were evaluated by reference to this data. The planar turbulent flow of a power-law fluid through a film bearing was calculated numerically by Pierre and Boudet (1985), but no comparisons were made with experimental data. These workers also closed the Reynolds stresses by analogy with the power-law model, but the eddy viscosity was determined using the low Reynolds number two-equation k–ε turbulence model of Lam and Bremhorst (LB) (1981).

Malin (1997) developed a low Reynolds number k–ε turbulence model exclusively for purely viscous power law fluids. His model was based on the Lam and Bremhorst (1981) damping function which he modified empirically by including the power index n but he gave no account of any effects of the non-linear

Received on April 25, 2005; accepted on July 20, 2005. Correspondence concerning this article should be addressed to J. B. Joshi (E-mail address: jbj@udct.org).

non-Newtonian viscosity on the turbulence model, except for the consideration of the power viscosity law for molecular diffusion terms. Malin's model only works for purely viscous fluids.

Cruz and Pinho (2003) developed a low Reynolds number model for predicting turbulent pipe flows of various polymer solutions. Their model was based on the Newtonian model of Nagano and Hishida (1987) with new viscous damping functions and one constant. The flow predictions compare favorably with the results from the experiment for mean velocity, but the kinetic energy predictions were not in agreement with the experimental data. A fairly complete review of the low Reynolds number k–ε model of the turbulent shear flows has been given by Patel *et al*. (1985), Hrenya *et al*. (1995) and Thakre and Joshi (2000, 2002). Thakre and Joshi (2000) have analyzed twelve different low Reynolds number k–ε models for the case of a single-phase pipe flow. For this purpose, they have used four criteria; accurate prediction of the radial variation of axial velocity, the turbulent kinetic energy and the eddy diffusivity (compared with the experimental data of Durst *et al*. (1995)). The fourth criterion was rather stringent and stipulated the necessary condition of the overall energy balance, i.e., the volume integral of ε must be equal to the energy-input rate (the pressure drop multiplied by the volumetric flow rate). All these four criteria were found to be satisfied by Lai and So (1990) (LSO) as shown by Thakre and Joshi (2000). In the present work, it was thought desirable to extend the work of Lai and So (1990) using Lai and So model. The aim of the work is to undertake a systematic study to investigate the effect of rheological parameters and to consider the modification to the flow that arises in the presence of a fluid yield stress. Further, it deals with the pipeline flow of time-independent viscous fluids described by the power-law rheological model, which relates the shear stress to the strain rate via the consistency index K and the power-law index n. For values of $n < 1$, the fluid is pseudoplastic (shear thinning), and for values of $n > 1$, it is dilatant (shear thickening). If $n = 1$ the fluid is Newtonian.

1. Mathematical Model

1.1 The transport equations

For steady, isothermal, incompressible, fully developed turbulent pipe flow, the set of governing equations for the flow are given as follows:

Momentum equation:

$$0 = \frac{1}{r}\left[\frac{\mathrm{d}}{\mathrm{d}r} r\left(\bar{\nu} + \nu_{\mathrm{T}}\right)\frac{\mathrm{d}u}{\mathrm{d}r}\right] - \frac{1}{\rho}\left(\frac{\mathrm{d}p}{\mathrm{d}z}\right)_{\mathrm{c}} \tag{1}$$

Transport equation for the turbulent kinetic energy (k)

$$0 = \frac{1}{r}\left[\frac{\mathrm{d}}{\mathrm{d}r} r\left(\bar{\nu} + \frac{\nu_{\mathrm{T}}}{\sigma_{\mathrm{k}}}\right)\frac{\mathrm{d}k}{\mathrm{d}r}\right] - \nu_{\mathrm{T}}\left(\frac{\mathrm{d}u}{\mathrm{d}r}\right)^2 - \varepsilon - D \tag{2}$$

Transport equation for the turbulent energy dissipation rate (ε) where,

$$0 = \frac{1}{r}\left[\frac{\mathrm{d}}{\mathrm{d}r} r\left(\left(\bar{\nu} + \frac{\nu_{\mathrm{T}}}{\sigma_{\varepsilon}}\right)\frac{\mathrm{d}\varepsilon}{\mathrm{d}r}\right)\right] + \frac{C_{\varepsilon 1} f_1 \nu_{\mathrm{T}} \varepsilon}{k}\left(\frac{\mathrm{d}u}{\mathrm{d}r}\right)^2 - \frac{C_{\varepsilon 2} f_2 \varepsilon^2}{k} + E \tag{3}$$

where,

$$\nu_{\mathrm{T}} = C_{\mu} f_{\mu} \frac{k^2}{\varepsilon} \tag{4}$$

and the apparent viscosity can be written as

$$\bar{\nu} = \frac{1}{\rho} K_{\mathrm{v}} \left[\dot{\gamma}^2\right]^{(n-1)/2} K_{\mathrm{e}} \left[\dot{\varepsilon}^2\right]^{(p-1)/2} \tag{5}$$

Since the viscosity is a non-linear function of fluctuating kinematics tensors it also fluctuates and this leads to the definition of average and fluctuating viscosities. An expression for the time averaged molecular viscosity at a high Re number was derived by Cruz and Pinho (2003) which is in a closed form once k and ε are known and given by

$$\bar{\mu}_{\mathrm{h}} = \left(C_{\mu}\rho\right)^{3m(m-1)A_2/\left[8+3m(m-1)A_2\right]} 2^{4m(m-1)A_2/\left[8+3m(m-1)A_2\right]} \cdot k^{6m(m-1)A_2/\left[8+3m(m-1)A_2\right]} \varepsilon^{\left[8-3m(m-1)A_2\right]m/\left[8+3m(m-1)A_2\right]} \cdot B^{8/\left[8+3m(m-1)A_2\right]} \tag{6}$$

The expression (Eq. (6)) was derived from arguments of high Reynolds number turbulence, the true average molecular viscosity is different near walls and at low Reynolds numbers. At a wall there are no velocity fluctuations, the flow is uni-directional, and the average viscosity must reduce to the pure viscometric form, i.e., without any extensional effect. To take this into account $\bar{\mu}_{\mathrm{h}}$ must be reduced by an appropriate molecular viscosity damping function f_{v}. Hence, the final expression for the average molecular viscosity

$$\bar{\mu} = f_{\mathrm{v}}\bar{\mu}_{\mathrm{h}} + \left(1 - f_{\mathrm{v}}\right)\eta_{\mathrm{v}} \tag{7}$$

The role of f_v is akin to that of the damping function for the eddy viscosity f_μ and it was decided to make $f_v = f_\mu$ after an extensive series of tests analyzed both the effects of $f_v > f_\mu$ and $f_v < f_\mu$ onto the predictions of the turbulence model. However, note that f_μ is not given by the standard Newtonian expression as it is affected by the new fluid rheology.

For Newtonian fluids there are many low Reynolds number k–ε models, which differ in the form of the extra terms and damping functions. Dhotre and Joshi (2004) have successfully extended this model to predict a heat transfer coefficient in low as well as high Prandtl number fluids. The model proposed by Lai and So (1990) has been chosen for its good performance in the Newtonian pipe flow. In Lai and So (1990)'s model the various extra terms and damping functions are:

$$f_1 = 1 + \left[1 - 0.6\exp\left(-\frac{Re}{10^4}\right)\right]\exp\left(-\left(\frac{R_T}{64}\right)^2\right) \tag{8}$$

$$f_2 = 1 - \frac{2}{9}\exp\left(-\left(\frac{R_T}{64}\right)^2\right) \tag{9}$$

$$E = 2\nu C_{\varepsilon 2} f_2 \frac{\varepsilon}{k}\left(\frac{\mathrm{d}\sqrt{k}}{\mathrm{d}r}\right)^2 + \exp\left(-\left(\frac{R_T}{64}\right)^2\right) \cdot \left[\left(\frac{7}{9}C_{\varepsilon 2} - 2\right)\frac{\varepsilon}{k}\left(\varepsilon - 2\nu\left(\frac{\mathrm{d}\sqrt{k}}{\mathrm{d}r}\right)^2 - \frac{1}{2k}\left(\varepsilon - \frac{2k\nu}{y}\right)^2\right)\right] \tag{10}$$

For our purpose, these four equations are all modified, with the average molecular kinematic viscosity-taking place of a constant kinematic viscosity. The damping function f_μ used by Lai and So (1990) is given by the following expression:

$$f_\mu = 1 - \exp\left(-0.0115y^+\right) \tag{11}$$

Where, in the low Reynolds number k–ε model, the function f_2 is introduced primarily to incorporate the low Reynolds effect in the destruction term of ε. The important criterion for the function f_2 is that, it should force the dissipation term in the ε equation to vanish at the wall. In the high Reynolds number flows, remote from the wall, the function f_1 asymptotes to the value of one in accordance with the high Reynolds number form of the model. The k–ε model parameters are: $C_\mu = 0.09$, $C_{\varepsilon 1} = 1.35$, $C_{\varepsilon 2} = 1.8$, $\sigma_k = 1$ and $\sigma_\varepsilon = 1.3$.

1.1.1 Viscosity damping functions All the low Re models adopt a damping function f_μ to account for the direct effect of molecular viscosity on the shear stress near the wall (viscous sub-layer and buffer zone). It may be noted that the wall functions used in connection with the standard k–ε model ($f_\mu = 1$) are usually applied in a region $y^+ > 30$. The damping function reduces the influence of the Reynolds shear stress on the total stress as the wall is approached, thus enhancing the influence of the molecular viscosity. In the wall region, the purely viscous stress contribution dominates the total stress in the momentum balance. The function f_μ should be modified for consistency with the adopted rheological equation and for that the Cruz and Pinho (2003)'s expression has been incorporated in the present work. To modify f_μ accounting the different fluid rheology, they used philosophy used by van Driest (1956) and derived functions $f_{\mu v}$ (viscometric damping function) and $f_{\mu e}$ (elongational damping function) for purely shear-thinning ($n < 1$) and purely Trouton-thickening fluids ($p > 1$), respectively. The damping function adopted in the present work is the product of $f_{\mu v}$ and $f_{\mu e}$. Cruz and Pinho (2003) finally came up with the following expression:

$$f_\mu = \left\{1 - \left[1 + \left|\frac{1-n}{1+n}\right| y^+\right]^{-\left|(1+n)/(1-n)\right|/A^+}\right\} \cdot \left\{1 - \left[1 + \left|\frac{p-1}{3-p}\right| y^+ C^{(1-p)/(2-p)}\right]^{-\left|(3-p)/(p-1)\right|/A^+}\right\} \tag{12}$$

Where, A^+ and C are the constants proposed by Cruz and Pinho (2003).

1.2 Boundary conditions

Since the flow is axisymmetric, only the boundary conditions at the wall and the symmetry line are required to be specified:

$$r = 0; \quad \frac{\mathrm{d}u}{\mathrm{d}r} = \frac{\mathrm{d}k}{\mathrm{d}r} = 0$$
$$r = R; \quad u = k = 0, \ \varepsilon_W = \nu\left(\mathrm{d}^2 k/\mathrm{d}y^2\right)_w \tag{13}$$

Equations (1)–(12), along with the boundary conditions (Eq. (13)), were solved.

1.3 Method of solution

The solution procedure is to solve the momentum equations to obtain the mean axial velocity, turbulent kinetic energy (k), and the turbulent energy dissipation rate (ε). The governing equations for the k–ε model are ordinary differential equations, and therefore can be solved by any iteration scheme for split boundary-value problems. A set of equations was solved numerically, which consisted of the following steps: (i) generation of grids, (ii) conversion of governing equations into algebraic equations, (iii) selection of discretization

Table 1 Numerical details

Reynolds number [s]	Number of grid points required (range)	Convergence criteria	Number of iteration required
4300	75–85	10^{-4}–10^{-5}	100–150
7442	75–85	10^{-4}–10^{-5}	100–150
16,600	75–85	10^{-4}–10^{-5}	100–200
22,000	85–150	10^{-4}–10^{-5}	200–250
42,900	85–150	10^{-4}–10^{-5}	200–250
45,300	85–150	10^{-4}–10^{-5}	200–250

scheme, (iv) formulation of discretized equations at every grid location and (v) development of a suitable iterative scheme for the use in obtaining a final solution. The finite control volume technique proposed by Patankar (1980) was used for solution of differential equations. Several discretization schemes (upwind, hybrid, exponential and the power law) were tested. Out of these, the second order UPWIND scheme was found to be the best and was used for discretization of the governing equations. The algebraic equations obtained after discretization were solved by a tri-diagonal matrix algorithm (TDMA). The grid generation is one of the important aspects of the numerical simulation. The robustness of any numerical code depends on effectiveness and the stability of the grid-generation scheme employed for the investigations. Thakre and Joshi (2001) have investigated the effect of the grid size in the range of 70–175. They have observed no effect when the grid size being beyond 100, and therefore, the same number was taken in this work. In the present work, non-uniform grids (in the range of 70–175) have been employed and more than half of the points have been located in the range of $r/R > 0.9$. The predictions obtained from this technique were found to be insensitive to the grids, since doubling the number of grid points changed the solution profiles by less than 1%. The numerical details have been given in the **Table 1**.

2. Results and Discussion

2.1 Comparison of numerical predictions with the experimental data

As a first step, it is important to establish the validity of the model for a Newtonian flow. Therefore, comparison has been made with the experimental data of Durst *et al.* (1995), Schildknecht *et al.* (1979), Eggels (1994) and details are given in Thakre and Joshi (2002). An excellent comparison result was obtained between the model predictions and the experimental data. For instance, **Figure 1** shows a typical case of such comparison for axial mean velocity and shear stress. The agreement between the predicted and the experimental data of Durst *et al.* (1995) seems excellent for the region $0.5 < y^+ < 100$. This Newtonian prediction was obtained with the same model and code by setting n and p equal to 1. This confirms the generality of the proposed turbulence model. In order to validate the low Reynolds number k–ε model for a different fluid, fully developed pipe flow measurements for shear thinning, drag reducing and shear thickening fluids

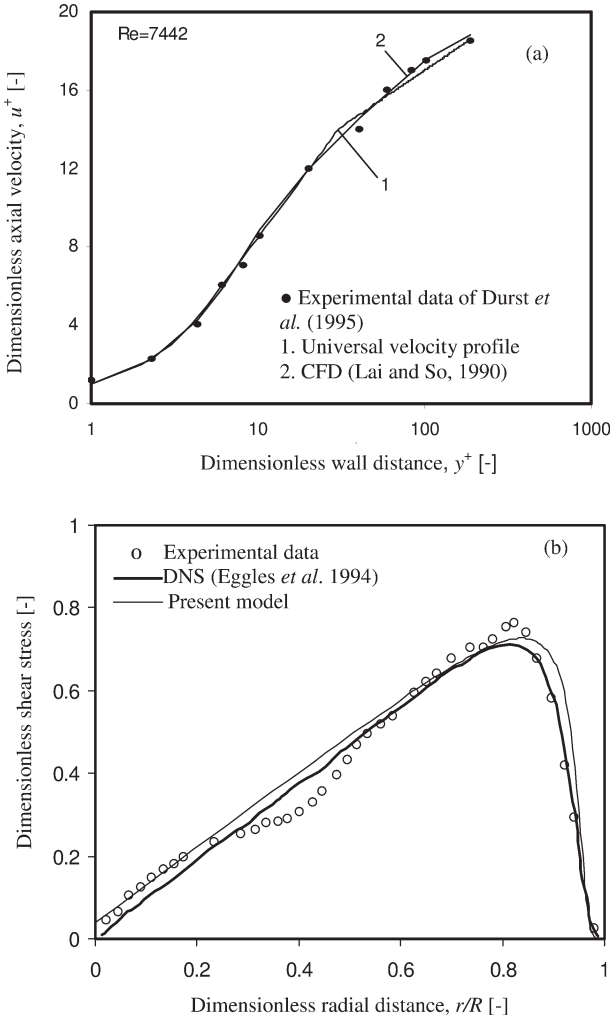

Fig. 1 Comparison of (a) velocity profile predictions and the experimental data of Durst *et al.* (1995) (Re = 7442) for universal velocity profile and the present CFD model; (b) stress profile with the experimental data of Eggels *et al.* (1994)

Table 2 Parameters of viscosity law Eqs. (3)–(7) used to fit the viscosity data

Fluid	K_v [Pa s^n]	n	K_e	p
0.25% CMC	0.2639	0.6174	2.0760	1.2678
0.3% CMC	0.2748	0.6377	2.7485	1.2214
0.4% CMC	0.2528	0.6177	0.9283	1.3982
0.09/0.09% CMC/XG	0.1518	0.5783	2.1833	1.1638
0.2% XG	0.2701	0.4409	3.8519	1.2592
0.125% PAA	0.2491	0.4250	8.2500	1.4796
0.2% PAA	0.7849	0.4075	9.8650	1.3175

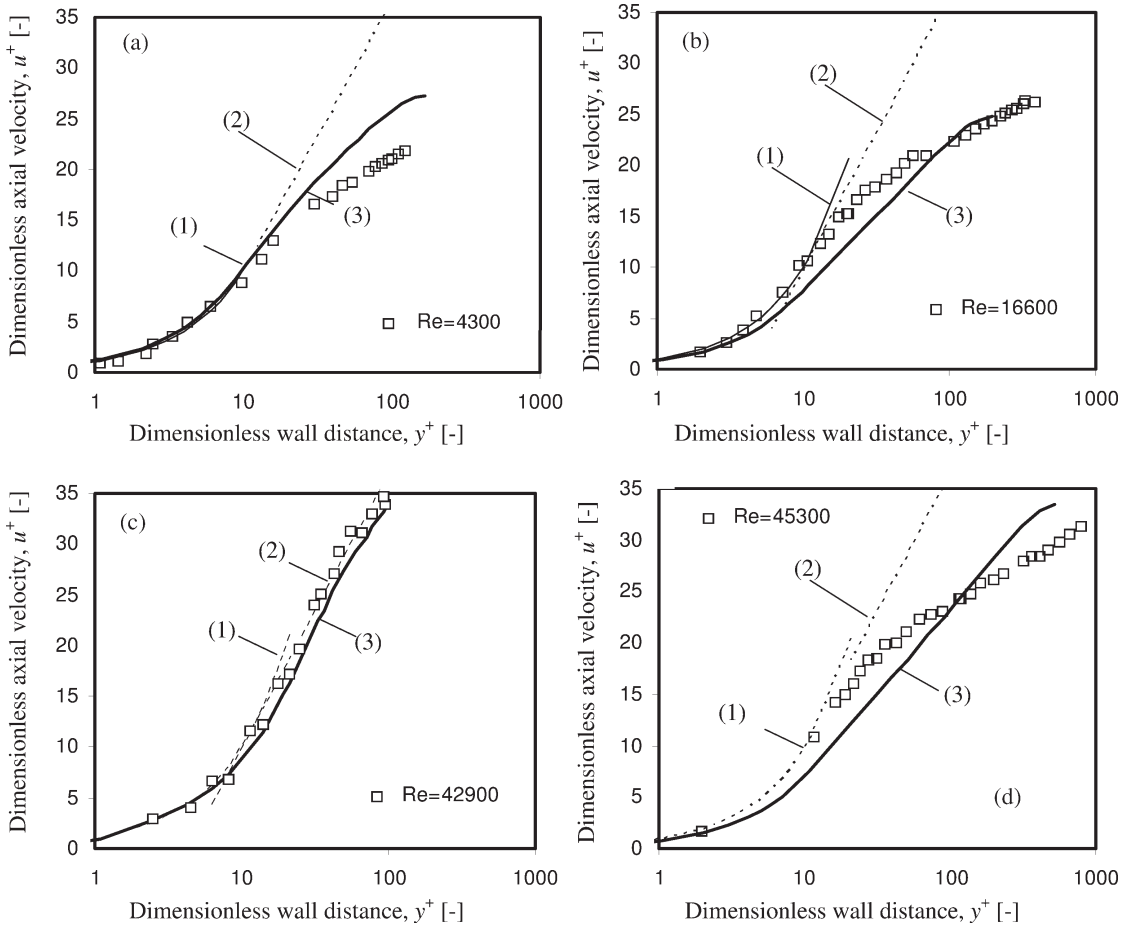

Fig. 2 Comparison of velocity profiles between CFD predictions and the experimental data of Escudier *et al*. (1998) for (a) 0.3% CMC solution (Re_w = 4300); (b) 0.25% CMC solution (Re_w =16,600); (c) 0.125% PAA (Re_w = 42,900); (d) 0.09/0.09% CMC/XG solution (Re_w = 45,300): (1) and (2), Virk's (1975) ultimate DR asymptote; (3), present CFD model

were chosen. In the present work, the experimental data of Escudier *et al*. (1998) and Presti (2000) for the drag reducing fluids have been used for validation. Their fluids were aqueous solutions of polyacrylamide (PAA), xanthan gum (XG), carboxymethyl cellulose (CMC) and a blend of XG and CMC at various weight concentrations. The corresponding parameters of viscosity laws are listed in **Table 2**.

2.2 Drag reducing fluids

Numerous studies have been undertaken to characterize drag reducing phenomena in polymer solutions. In fact addition of very low concentrations of dissolved polymers can reduce frictional resistance in the turbulent flow to as low as one quarter of that of the pure solvent, making the phenomena potentially very important. In view of this, simulations have been

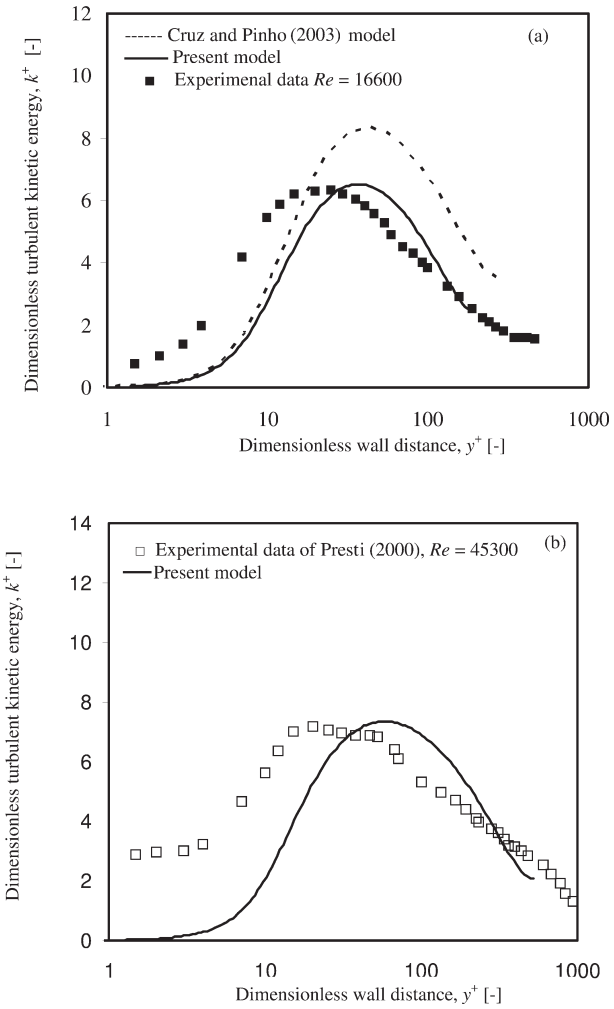

Fig. 3 Comparison of predicted kinetic energy with the experimental data of Presti (2000) for (a) 0.25% CMC solution (Re_w = 16,600); (b) 0.09/0.09% CMC/XG (Re_w = 45,300)

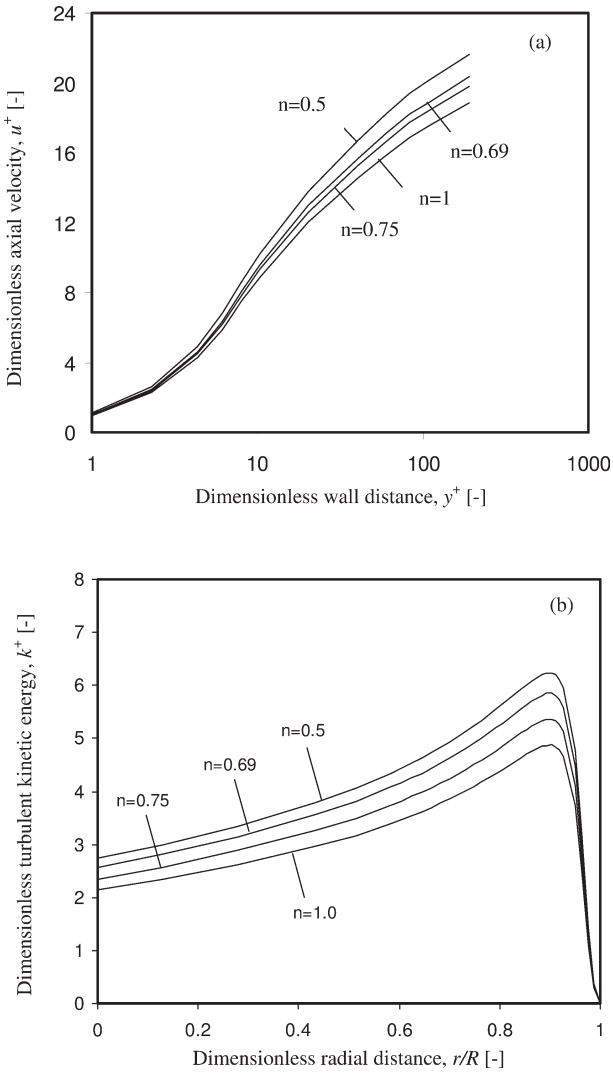

Fig. 4 Effect of shear behavior exponent n on (a) turbulent mean velocity profiles for Re = 7442; (b) turbulent kinetic energy profiles for Re = 22,000

carried out for drag reducing fluids. **Figures 2**(**a**)–(**d**) shows a comparison between CFD predictions and the experimental velocity profile by Escudier *et al*. (1998) for different drag reducing fluids.

Figure 2(a) shows a comparison between CFD predictions under Re = 4300 for the 0.3%CMC solution with the experimental data. Figure 2(b) shows comparison between CFD prediction for Re = 16,600 for the 0.25% CMC solution with experimental data. Figure 2(c) shows comparison between CFD prediction for Re = 42,900 for the 0.125% PAA solution with the experimental data. Figure 2(d) shows comparison between CFD prediction for Re = 45,300 for 0.09/0.09% CMC/XG solution with the experimental data. All these figures include the CFD predictions, the experimental data and Virk's (1975) ultimate DR asymptote. It can be seen that the model predictions are in fairly good agreement with the experimental data.

The CFD predictions of turbulent kinetic energy have been given in **Figures 3**(**a**) and (**b**) with the experimental data of Presti (2000) when Re = 16,600 for a blend of 0.259% CMC and when Re = 45,300 for a blend of 0.09/0.09% CMC/XG, respectively. The characteristic turbulent kinetic energy profile for a Newtonian fluid consists of a rapid increase from zero on the wall to a maximum peak located in the region y^+ = 20 followed by a progressive decay down to the centre of the pipe. The experiments show that the peak turbulence for a drag reducing fluid is always higher than that for a Newtonian fluids but it is located farther away from the wall. It can also be noted that in the ineterial layer the turbulent kinetic energy is well predicted by the Lai and So model as compared to Cruz and Pinho (2003) model.

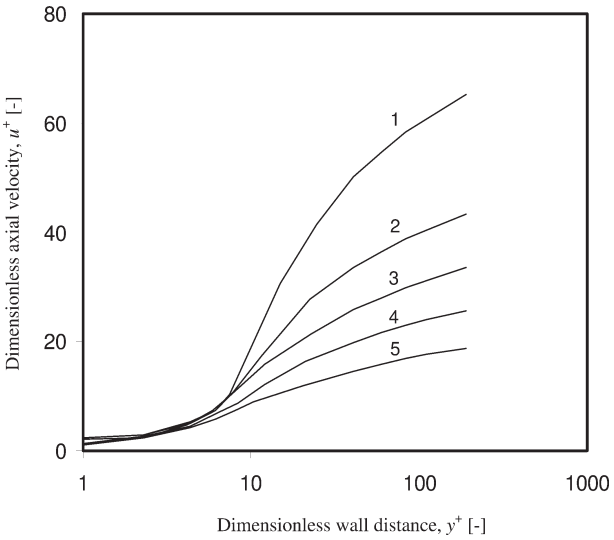

Fig. 5 Effect of Trouton ratio hardening exponent p on predictions of the velocity profile for constant shear viscosity fluids (n = 1) Re_W = 40,000: (1) p = 1.8; (2) p = 1.6; (3) p = 1.4; (4) p = 1.2; (5) p = 1.0

2.3 Shear thinning and shear thickening fluids

Figures 4(**a**) and (**b**) shows the effect of n on the velocity profile and the turbulent kinetic energy profile when Re = 7442, respectively. It can be seen from Figure 4(a) that the thickness of the viscous sub-layer reduces with decreasing n and the velocity profiles become progressively flatter owing to the increase in apparent viscosity, and hence the turbulence diminishes over the entire pipe cross section. It can be observed that as the index n increases, the profiles for the power law fluid approach the Newtonian profile as expected. The results for n = 0.5 fall sufficiently for the Newtonian profile to suggest that this flow might be transitional. For n = 1 the CFD predictions agree with the data from the literature for Newtonian fluids and model becomes identical to Lai and So's (1990) low Reynolds number model. Figure 4(b) shows the effect of the power-law index on the turbulence kinetic energy profiles at Re = 7442. It can be seen that in addition to narrowing of the viscous sub layer, there is also pronounced attenuation of the turbulence with a decreasing power-law index.

Figure 5 shows the effect of strain-hardening of the extensional viscosity on predictions of the velocity profile for constant shear viscosity fluids. It can be observed that as p increases the velocity profile shifts from the Newtonian behavior and it exceeds further as for p = 1.8, the data of which are close to that for a laminar flow.

Conclusions

1. Difficulties encountered in experimentation as a result of using polymer solutions for approximation idealized rheologies can cause problems in interpretation and understanding. Application of the CFD to flows of non-Newtonian fluids with a rheological certainty under study has a potential to correctly quantify and understand the effect of different rheological parameters.
2. The modified version of Lai and So (1990) low Reynolds number k–ε model has been used to predict the liquid velocities and the turbulent viscosity for the drag reducing fluid, a non-Newtonian fluid. The comparison between the predictions and the experimental profiles of axial velocity and turbulent kinetic energy are in good agreement. The model also establishes a good energy balance.

Nomenclature

A^+	=	constant used in Eq. (12)	[—]
CFD	=	computational fluid dynamics	[—]
C	=	constant in Eq. (12)	[—]
C_μ, $C_{\varepsilon 1}$, $C_{\varepsilon 2}$	=	turbulence parameters in the k–ε model	[—]
C_P	=	specific heat at a constant pressure	[kJ kg^{-1} °C^{-1}]
D	=	term contained in the k equation	
$(dp/dz)_c$	=	constant axial pressure gradient	[—]
E	=	term contained in the ε equation	
f	=	friction factor	[—]
f_μ, f_1, f_2	=	damping functions used in low Reynolds number k–ε and Reynolds stress models	[—]
K_e	=	viscosity consistency index of Trouton ratio behavior	[—]
K_v	=	viscosity consistency index of shear behavior	[—]
k	=	turbulent kinetic energy	[m^2 s^{-2}]
k^+	=	normalised turbulent kinetic energy, $=k/u_\tau^2$	[—]
m	=	parameter defined in Eq. (6)	[—]
n	=	viscosity power index of shear behaviour	[—]
p	=	viscosity power index of Trouton ratio behaviour	[—]
r	=	radial component	[m]
R	=	radius of a pipe	[m]
Re	=	Reynolds number based on mean velocity, $=2Ru/\nu$	[—]
Re^*	=	Reynolds number based on friction velocity, $=Ru_\tau/\nu$	[—]
R_T	=	turbulent Reynolds number, $=k^2/\nu\varepsilon$	[—]
R_y	=	turbulent Reynolds number based on y, $=\sqrt{k}\,y/\nu$	[—]
Re_W	=	wall Reynolds number, $=Ru_\tau/\nu_W$	[—]
u	=	axial velocity	[m s^{-1}]
u^+	=	normalised mean axial fluid velocity, $=u/u_\tau$	[—]
u_b	=	bulk mean axial velocity of fluid	[m s^{-1}]
u_τ	=	friction velocity, $=\sqrt{-R(dp/dz)_c/(2\rho)}$	[m s^{-1}]
y	=	normal distance from the wall, $=R-r$	[m]
y^+	=	dimensionless wall distance, $=yu_\tau/\nu$	[—]
z	=	axial co-ordinate	[m]
ε	=	turbulent energy dissipation rate	[m^2 s^{-3}]
ε_w	=	turbulent energy dissipation rate on the wall	[m^2 s^{-3}]
μ	=	molecular viscosity of a fluid	[kg m^{-1} s^{-1}]
$\bar{\mu}_h$	=	time averaged molecular viscosity due to high Reynolds number	[kg m^{-1} s^{-1}]
μ_t	=	turbulent viscosity of a fluid	[kg m^{-1} s^{-1}]
ρ	=	density of liquid	[kg m^{-3}]
ν	=	molecular kinematic viscosity of a liquid	[m^2 s^{-1}]
$\bar{\nu}$	=	average kinematic viscosity	[m^2 s^{-1}]
ν_T	=	eddy diffusivity of liquid	[m^2 s^{-1}]

σ_k = turbulent Prandtl number for k [—]
σ_ε = turbulent Prandtl number for ε [—]

Literature Cited

Bogue, D. C.; "Entrance Effects and Prediction of Turbulence in Non-Newtonian Flow," *Ind. Eng. Chem.*, **51**, 874–878 (1959)

Cruz, D. O. A. and F. T. Pinho; "Turbulent Pipe Flow Predictions with a Low Reynolds Number k–ε Model for Drag Reducing Fluids," *J. Non-Newtonian. Fluid Mech.*, **114**, 109–148 (2003)

Dhotre, M. T. and J. B. Joshi; "CFD Simulation of Heat Transfer in Turbulent Pipe Flow," *Ind. Eng. Chem. Res.*, **43**, 2816–2829 (2004)

Dodge, D. W. and A. B. Metzner; "Turbulent Flow of Non-Newtonian Systems," *AIChE J.*, **5**, 189–204 (1959)

Durst, F., J. Jovonavic and J. Sender; "LDA Measurement in the Near Wall Region of Turbulent Pipe Flow," *J. Fluid Mech.*, **295**, 305–335 (1995)

Eggels, J. G. M., F. Unger, M. H. Weiss, J. Westerweel, R. J. Adrian, R. Friedrich and F. T. M. Nieuwstadt; "Fully Developed Turbulent Pipe Flow: A Comparison of Direct Numerical Simulation and Experiments," *J. Fluid Mech.*, **268**, 175–209 (1994)

Escudier, M. P., F. Presti and S. Smith; "Drag Reduction in the Turbulent Pipe Flow of Polymers," *J. Non-Newtonian Fluid Mech.*, **81**, 197–213 (1998)

Hartnett, J. P. and M. Kostic; "Turbulent Friction Factor Correlations for Power Law Fluids in Circular and Non-Circular Channels," *Int. Commun. Heat Mass Transfer*, **17**, 59–65 (1990)

Hrenya, C. M., E. J. Bolio, D. Chakrabarti and J. L. Sinclair; "Comparison of Low Reynolds Number k–ε Turbulence Models in Predicting Fully Developed Pipe Flow," *Chem. Eng. Sci.*, **50**, 1923–1941 (1995)

Lai, Y. G. and R. M. C. So; "On Near Wall Turbulent Flow Modeling," *J. Fluid Mech.*, **221**, 641–673 (1990)

Lam, C. K. G. and K. Bremhorst; "A Modified Form of the k–ε Model for Predicting Wall Turbulence," *J. Fluids Eng.*, **103**, 456–460 (1981)

Malin, M. R.; "Turbulent Pipe Flow of Power-Law Fluids," *Int. Commun. Heat Mass Transfer*, **24**, 977–988 (1997)

Metzner, A. B.; "Non-Newtonian Fluid Flow. Relationships between Recent Pressure-Drop Correlations," *Ind. Eng. Chem.*, **49**, 1429–1432 (1957)

Metzner, A. B. and J. C. Reed; "Flow of Non-Newtonian Fluids-Correlation of the Laminar, Transition and Turbulent Flow Regions," *AIChE J.*, **1**, 434–440 (1955)

Mohammed, A. L. Y., N. N. Gubaji and P. R. Smith; *ASCE J. Hyd. Div.*, HY7, 885 (1975)

Nagano, Y. and M. Hishida; "Improved Form of the k–ε Model for Wall Turbulent Shear Flows," *J. Fluids Eng.*, **109**, 156–160 (1987)

Patankar, S. V.; Numerical Heat Transfer and Fluid Flow, McGraw-Hill, New York, U.S.A. (1980)

Patel, V. C., W. Rodi and G. Scheuerer; "Turbulence Models for Near Wall and Low Reynolds Number Flows," *AIAA J.*, **23**, 1308–1319 (1985)

Pierre, J. F. and R. Boudet; Laminar and Turbulent Flows, 4th Int. Conf. Num. Meth., p. 235, Pineridge Press, Swansea, U.K. (1985)

Presti, F.; Investigation of Transitional and Turbulent Pipe Flow of Non-Newtonian Fluids, Ph.D. Thesis, University of Liverpool, U.K. (2000)

Reed, T. D. and A. A. Pilehvari; SPE 25456, Prod. Operations Symp. 39, Oklahoma City, U.S.A. (1993)

Schlichting, H.; Boundary Layer Theory, 6th ed., J. Kestin translated, McGraw-Hill, New York, U.S.A. (1968)

Schildknecht, M., J. A. Miller and G. E. A. Meir; "The Influence of Suction on the Structure of Turbulence in Fully Turbulent Pipe Flow," *J. Fluid Mech.*, **90**, 67–107 (1979)

Thakre, S. S. and J. B. Joshi; "CFD Modeling of Heat Transfer in Turbulent Pipe Flows," *AIChE J.*, **46**, 1798–1812 (2000)

Thakre, S. S. and J. B. Joshi; "A Low Reynolds Number k–ε Modelling of Turbulent Pipe Flow: Patterns and Energy Balance," *Can. J. Chem. Eng.*, **79**, 214–226 (2001)

Thakre, S. S. and J. B. Joshi; "Momentum, Mass and Heat Transfer in Single Phase Turbulent Flow," *Rev. Chem. Eng.*, **18**, 83–293 (2002)

Van Driest, E. R.; "On Turbulent Flow Near a Wall," *J. Aeronaut. Sci.*, **23**, 1007–1011 (1956)

Virk, P. S.; "Drag Reduction Fundamentals," *AIChE J.*, **21**, 625–656 (1975)